Millimeter Wave Adaptive Transmission Using Spatial Scattering Modulation

Ding, Y.; Kim, K.J.; Koike-Akino, T.; Pajovic, M.; Wang, P.; Orlik, P.V.

TR2017-045 May 2017

Abstract

In millimeter wave (mmWave) communication, analog and hybrid beamforming systems are proposed to reduce the number of RF chains when a large antenna array is utilized to achieve a high beamforming gain. In this paper, a new transmission scheme is first proposed by leveraging the hardware architecture of analog and hybrid beamforming to improve the spectral efficiency. The new scheme is called spatial scattering modulation (SSM), since it exploits the spatial scattering dimension to modulate information bits. And then, an adaptive transmission strategy (ATS) which chooses the best transmission scheme under instantaneous channel state information, is proposed to improve the performance. Link-level simulation results demonstrate the superiority of the proposed ATS in all the simulated signal-to-noise (SNR) values.

IEEE International Conference on Communications (ICC)

Millimeter Wave Adaptive Transmission Using Spatial Scattering Modulation

Yacong Ding
Department of Electrical and Computer Engineering
University of California, San Diego
La Jolla, California 92093
Email: yad003@ucsd.edu

Kyeong Jin Kim, Toshiaki Koike-Akino,
Milutin Pajovic, Pu Wang, and Philip Orlik
Mitsubishi Electric Research Laboratories
201 Broadway, Cambridge, Massachusetts 02139
{kkim,koike,pajovic,pwang,porlik}@merl.com

***Abstract*—In millimeter wave (mmWave) communication, analog and hybrid beamforming systems are proposed to reduce the number of RF chains when a large antenna array is utilized to achieve a high beamforming gain. In this paper, a new transmission scheme is first proposed by leveraging the hardware architecture of analog and hybrid beamforming to improve the spectral efficiency. The new scheme is called *spatial scattering modulation* (SSM), since it exploits the spatial scattering dimension to modulate information bits. And then, an adaptive transmission strategy (ATS) which chooses the best transmission scheme under instantaneous channel state information, is proposed to improve the performance. Link-level simulation results demonstrate the superiority of the proposed ATS in all the simulated signal-to-noise (SNR) values.**

***Index Terms*—Millimeter-wave, spatial scattering modulation, hybrid transmission.**

I. Introduction

As the increasing demand for high data rates, millimeter wave (mmWave) radio bands have been attracting more attention since they provide enormous amount of bandwidth which is essential in achieving multigigabit data rates. However, a high path loss has arisen in using mmWave for indoor and outdoor transmissions system. To deal with this, a highly directional beamforming has been proposed, which has been possible by using a large number of antenna elements in a fixed physical aperture size.

Depending on the hardware architecture, three types of beamforming can be categorized, namely, digital, analog, and hybrid [1], [2]. Digital beamforming requires that each antenna element is connected to its own radio frequency (RF) chain, whereas analog and hybrid beamforming require that each RF chain is connected to the antenna array via a phase shifter array. When the antenna array is large, it is impractical to apply digital beamforming due to high hardware cost and power consumption of RF chains. Thus, analog and hybrid beamforming systems are more reasonable choices in mmWave communications systems.

To reduce the number of RF chains, the spatial modulation (SM) [3], [4] has been proposed. In the conventional SM, the spatial position of the antenna at the transmitter has been mainly used to send additional information bits through a wireless fading channel. Comparing with the closed-loop transmit antenna selection (TAS) [5], an antenna switching in the SM depends on the information bit. Since only one antenna is activated at any transmission time, inter-channel interference can be removed from the received signal. Also, a tight intra-antenna synchronization is not required [6]. The SM concept has also been generalized such that more than one antennas are activated to encode information [7], and extended to the large antenna array scenario [8]. An alternative multiple-input multiple-output (MIMO) transmission [9] has been proposed. At symbol time instance, a radiation pattern is changed. Input information bits are encoded onto angular variations of the far-field in the wave-vector domain. A similar concept which applies index modulation (IM) [10], [11] has been proposed for Orthogonal Frequency Division Multiplexing (OFDM) transmission, namely OFDM-IM transmission scheme. By employing the IM, only a set of subcarriers is selected by information bits for transmission, so that the remaining subcarriers are inactive for transmission. It has been shown from [10], [11] that OFDM-IM can have a better error rate performance over a classical OFDM transmission scheme for a low-to-mid spectral efficiency range.

Motivated by the work in the SM and OFDM-IM, we propose a new modulation, namely spatial scattering modulation (SSM). In this modulation, we exploit the degrees of freedom in the spatial angle domain of the scattering clusters. One spatial angle steering to a single scattering cluster is determined by the information bits, and this angle is used to form a directional beam. A modulated symbol is then transmitted towards this direction by beamforming. Due to full use of a large antenna array, we are able to form a very fine spatial resolution as well as a highly directional beam with a very narrow beam width. This facilitates beamforming towards a specific scattering cluster. Notice that we consider the non-line-of-sight (NLOS) scenario in our scheme, which is common for the outdoor mmWave transmission [12], [13].

An adaptive transmission strategy (ATS) is also proposed to improve the performance. At each transmission time, one transmission scheme out of full-SSM (FSSM), partial-SSM (PSSM), and maximum beamforming (MBF), which provides the best conditional bit error rate will be chosen. Since this ATS uses an optimal transmission instantaneously, a better

Yacong Ding's work was performed during his internship at Mitsubishi Electric Research Labs, Cambridge, MA.

BER can be promised. The link-level simulations demonstrate the superiority of the ATS over the other non-adaptive transmission schemes.

A. Organization

This paper is organized as follows. Section II introduces the hardware architecture and channel model used in the paper, and basic concept of SSM. In Section III, we propose the ATS, which chooses the best transmission scheme instantaneously based on the theoretical bound of the conditional bit error rate. Section IV presents some simulation results and we conclude the paper in Section V.

B. Notation

$\mathcal{CN}(\mu, \sigma^2)$ and $\mathcal{N}(\mu, \sigma^2)$, respectively, denote the complex and real Gaussian distributions with mean μ and variance σ^2.

II. Spatial Scattering Modulation

A. System and Channel Model

In the proposed system, we adopt analog and hybrid beamforming [1], [2] as shown in Fig. 1. In this adoption, we have considered hardware cost and power consumption, meanwhile leveraging a large antenna array to achieve a high beamforming gain. In analog and hybrid beamforming, each RF chain is connected to all antenna elements in the array through a set of phase shifters. We consider uplink transmission, where the user terminal (UT) acts as the transmitter, and the base station (BS) acts as the receiver. The UT has N_t antenna elements in the antenna array and we assume that it has limited power and fabrication cost budget, so that the UT has only one RF chain. In contrast, the BS has N_r antennas in its antenna array and R RF chains. We assume $R \geq 1$ due to a more powerful hardware resource at the BS. Since the UT has only one RF chain, it can only transmit a single stream and perform analog beamforming that steers to the dominant path direction [1] to achieve a high beamfoming gain. In contrast, when the receiver has multiple RF chains ($R \geq 2$), it can use any receiver combine method proposed in [14].

We adopt a narrowband discrete channel model proposed in [13], [15]. Also, we assume that exact channel state information (CSI) is available in the system. The channel matrix $\boldsymbol{H} \in \mathbb{C}^{N_r \times N_t}$ is assumed to be a sum of N_{ts} paths, written as:

$$\boldsymbol{H} = \sum_{l=1}^{N_{ts}} \beta_l \boldsymbol{a}_r(\theta_l^r) \boldsymbol{a}_t^H(\theta_l^t) \tag{1}$$

where β_l is the gain of the lth path, and θ_l^r and θ_l^t are azimuth angles of arrival (AOA) and angles of departure (AOD), respectively. We assume that both the UT and BS utilize a uniform linear array (ULA), so that the array manifold vectors $\boldsymbol{a}_r(\theta_l^r)$ and $\boldsymbol{a}_t^H(\theta_l^t)$ can be written as [16]:

$$\boldsymbol{a}_r(\theta_l^r) = \frac{1}{\sqrt{N_r}} \left[1, e^{j2\pi\psi_l^r}, e^{j2\pi\psi_l^r \cdot 2}, \ldots, e^{j2\pi\psi_l^r \cdot (N_r-1)}\right]^T,$$
$$\boldsymbol{a}_t(\theta_l^t) = \frac{1}{\sqrt{N_t}} \left[1, e^{j2\pi\psi_l^t}, e^{j2\pi\psi_l^t \cdot 2}, \ldots, e^{j2\pi\psi_l^t \cdot (N_t-1)}\right]^T$$

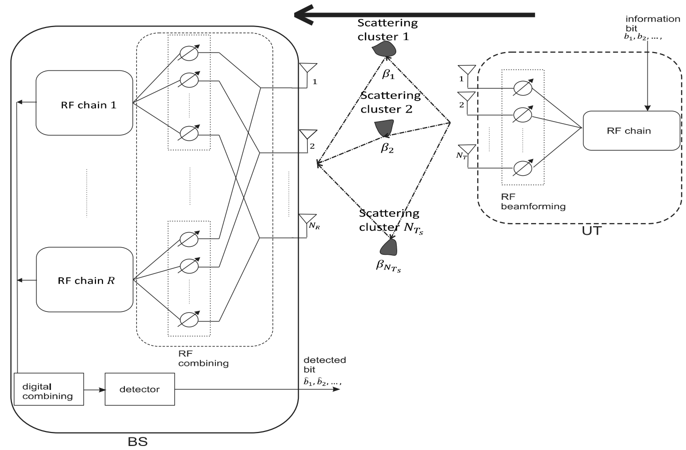

Fig. 1: Simplified architecture of the transmitter and receiver in uplink communications, where β_l denotes the gain of the lth scattering cluster.

where $\psi_l^r \stackrel{\triangle}{=} \frac{d_r}{\lambda}\sin(\theta_l^r)$ and $\psi_l^t \stackrel{\triangle}{=} \frac{d_t}{\lambda}\sin(\theta_l^t)$, d_r, d_t denotes antenna spacing at the BS and UT, respectively, λ is the wavelength of the propagation. The employed channel model is a simplified version of the clustered channel model in [13], such that we use a representative path to express the total effects of all paths in a cluster. When N_r and N_t is large, which is the typical assumption in mmWave transmission systems, we have $\boldsymbol{a}_r(\theta_l^r)^H \boldsymbol{a}_r(\theta_k^r) \approx 0, l \neq k$ and $\boldsymbol{a}_t(\theta_l^t)^H \boldsymbol{a}_t(\theta_k^t) \approx 0, l \neq k$ [13], [15], [16]. Since transmit and receiver beams can be narrow interference among scattering clusters is limited. Based on the knowledge in above, we assume an exact orthogonality among all AOA's and AOD's in this paper:

$$\boldsymbol{a}_r(\theta_l^r)^H \boldsymbol{a}_r(\theta_k^r) = \delta(l-k), \boldsymbol{a}_t(\theta_l^t)^H \boldsymbol{a}_t(\theta_k^t) = \delta(l-k) \tag{2}$$

where $\delta(\cdot)$ denotes the Dirac delta function. We also make idealized assumption that accurate channel state information is available at both transmitter and receiver in order to demonstrate the proposed SSM schemes and simplify the theoretical calculations. We leave the development of practical channel estimation algorithm as well as performance analysis under non-orthogonal AOA/AOD and imperfect channel estimation for the future work.

B. SSM Transmission

Due to the adopted architecture in Fig. 1, where the UT has only one RF chain, the UT can transmit to only one direction at each transmission time, i.e., steering to only one scattering cluster. Instead of steering to the cluster that has the largest gain β_l, SSM makes the UT to choose N_s clusters having largest gains out of N_{ts} clusters as candidate transmission clusters. Denote the transmitted symbol as s which has a normalized energy and is selected from M-ary constellations. Also, $\boldsymbol{p}$ as the transmission direction with unit norm $\|\boldsymbol{p}\|_2 = 1$. Given an independent information bit stream $[b_1, b_2, b_3, b_4, \ldots]$, SSM works as follows:

- Use $\log_2(N_s)$ information bits to determine which scattering clusters is selected for transmission.

- Use next $\log_2(M)$ information bits to determine which constellation point is chosen from M-ary constellations.

Then, the received signal at the receiver antenna array is given by

$$\boldsymbol{y} = \sqrt{E}\boldsymbol{H}\boldsymbol{p}s + \boldsymbol{n} \tag{3}$$

where E is the transmission energy, and $\boldsymbol{n} \sim \mathcal{CN}(\mathbf{0}, \sigma^2\mathbf{I}_{N_r})$ is the noise at receiver antennas.

As one example of SSM, let us assume that the UT chooses $N_s = 4$ scattering clusters as candidate transmission clusters, and uses QPSK $M = 4$ for symbol modulation. Without loss of generality, we assume that the scattering clusters are indexed with decreasing order of magnitude in such a way that $|\beta_1| > |\beta_2| > \ldots > |\beta_{N_{ts}}|$. Based on two information input bits $[b_1, b_2]$, one transmission direction vector $\boldsymbol{p}$ steering to one cluster is determined. Based on the next two bits $[b_3, b_4]$, one QPSK-modulated symbol is generated. The transmission direction vector and the modulated symbols are generated according to the following table.

$[b_1, b_2]$	00	01	10	11
$\boldsymbol{p}$	$\boldsymbol{a}_t(\theta_1^t)$	$\boldsymbol{a}_t(\theta_2^t)$	$\boldsymbol{a}_t(\theta_3^t)$	$\boldsymbol{a}_t(\theta_4^t)$
$[b_3, b_4]$	00	01	10	11
s	$\frac{(1+1j)}{\sqrt{2}}$	$\frac{(1-1j)}{\sqrt{2}}$	$\frac{(-1+1j)}{\sqrt{2}}$	$\frac{(-1-1j)}{\sqrt{2}}$

Thus, as one example of the input bit stream $[b_1, b_2, b_3, b_4] = [1\,1\,0\,0]$, the received signal is evaluated as follows:

$$\boldsymbol{y} = \sqrt{E}\boldsymbol{a}_r(\theta_4^r)\beta_4\frac{(1+1j)}{\sqrt{2}} + \boldsymbol{n} \tag{4}$$

where we have used (2) in the computation of (4).

C. SSM Detection

The BS receives $\boldsymbol{y}$ and combines it using its phase shifter arrays. Since there is no interference among scattering clusters as in (2), and only one stream is transmitted from the UT, from (4), the optimal combiner will be the maximal ratio combining that steers its beam towards the cluster used by transmit beamforming. However, there are N_s clusters and the BS has no knowledge about which one was actually used. With the constraint that $N_s \leq R$, the BS can utilize its R sets of phase shifter arrays, each one steering to one candidate scattering cluster. Thus, the combined signal is given by

$$\boldsymbol{y}_c = \begin{bmatrix} \boldsymbol{a}_r(\theta_1^r)^H \\ \vdots \\ \boldsymbol{a}_r(\theta_{N_s}^r)^H \end{bmatrix}\boldsymbol{y}. \tag{5}$$

Note that if there are more scattering clusters in the environment than the number of RF chains in the BS, i.e., $N_{ts} \geq R$, then the UT can choose up to R scattering clusters to perform SSM.

With the combined signal $\boldsymbol{y}_c$, maximum likelihood (ML) detection is performed to determine which cluster or direction and what constellation point were used at the UT as:

$$\{\hat{k}, \hat{s}\} = \underset{s,k\in\{1,\ldots,N_s\}}{\arg\min} |\boldsymbol{y}_c(k) - \boldsymbol{a}_r(\theta_k^r)^H\boldsymbol{H}\boldsymbol{a}_t(\theta_k^t)\sqrt{E}s|^2 \tag{6}$$

where $\boldsymbol{y}_c(k)$ denotes the kth element of $\boldsymbol{y}_c$. Equation (6) shows that we need to detect both transmission direction k and transmitted symbol s since both of them were used by information bits. Especially, $\hat{k}$ reveals the first $\log_2(N_s)$ bits, and $\hat{s}$ reveals the next $\log_2(M)$ bits.

III. Adaptive Transmission Strategy

Since $\beta_1, \ldots, \beta_{N_s}$ represent small scale fading and change from one time instant to another, the environment will favor a different transmission scheme at different transmission time. The best transmission scheme in minimizing the BER can be determined instantaneously. Assuming that both UT and BS can track β_l, and if we can quantify the performance metric of different transmission schemes based on instantaneous β_l, we can adaptively choose the scheme that provides the best performance. Based on this concept, we propose the ATS that computes the conditional bit error rate (CBER) based on instantaneous β_l, and chooses the transmission scheme with the smallest CBER at each transmission time. The ATS can achieve an instantaneous optimal performance, which leads to the optimal performance also in average sense. In the following, we specify three transmission schemes, full SSM (FSSM), partial SSM (PSSM) and maximal beamforming (MBF), the ATS will choose instantaneously the best one among them.

A. FSSM and PSSM

For FSSM, the transmitter utilizes all the N_s ($N_s \leq R$) directions for transmission. Assume the spectral efficiency of the system is S bits per transmission, therefore for FSSM the first $\log_2(N_s)$ bits are utilized to specify a direction for transmission, and the remaining $S - \log_2(N_s)$ bits are used for symbol modulation. In contrast, for PSSM we only utilize part of N_s directions for transmission. Denote N_s' as number of directions used in PSSM, where $N_s' < N_s$, and is typically chosen as power of two. PSSM will choose from directions corresponding to $\beta_1, \ldots, \beta_{N_s'}$. The first $\log_2(N_s')$ bits are used for specifying a direction and the next $S - \log_2(N_s')$ bits for symbol modulation. For example, consider a target spectral efficiency of $S = 4$ and four RF chains at the BS. FSSM chooses $N_s = 4$ largest scattering clusters and uses $\log_2(N_s) = 2$ bits for specifying a direction and $S - \log_2(N_s) = 2$ bits for QPSK modulation. PSSM chooses from $N_s' = 2$ largest scattering clusters and uses $\log_2(N_s') = 1$ bits for choosing a direction and $S - \log_2(N_s') = 3$ bits for 8QAM modulation. Thus, at the same spectral efficiency, PSSM uses a higher modulation order than FSSM in general.

B. CBER for SSM

When channel gains $\beta_l, l = 1, \ldots, N_s$ are given, assume k^* and s^* are the true transmission direction and transmitted symbol, and $\hat{k}$ and $\hat{s}$ are detected direction and symbol using criterion in (6), then the conditional pairwise error probability (CPEP) is given by

$$\mathbb{P}\big(\{k^*, s^*\} \to \{\hat{k}, \hat{s}\} \mid \beta_1, \ldots, \beta_{N_s}\big) = \mathbb{P}\big(|\boldsymbol{y}_c(k^*) - \boldsymbol{a}_r(\theta^r_{k^*})^H \boldsymbol{H}\boldsymbol{a}_t(\theta^t_{k^*})\sqrt{E}s^*|^2 > |\boldsymbol{y}_c(\hat{k}) - \boldsymbol{a}_r(\theta^r_{\hat{k}})^H \boldsymbol{H}\boldsymbol{a}_t(\theta^t_{\hat{k}})\sqrt{E}\hat{s}|^2\big). \quad (7)$$

According to the orthogonality provided in (2), for $k = k^*$ or $\hat{k}$ and $s = s^*$ or $\hat{s}$, we have

$$\boldsymbol{y}_c(k) = \boldsymbol{a}_r(\theta^r_k)^H \boldsymbol{y} = \begin{cases} \boldsymbol{a}_r(\theta^r_k)^H \boldsymbol{n}, & k \neq k^* \\ \beta_{k^*}\sqrt{E}s^* + \boldsymbol{a}_r(\theta^r_{k^*})^H \boldsymbol{n}, & k = k^*. \end{cases}$$

Thus, (7) can be simplified as (8) at the top of the next page. To evaluate CPEP, we need to analyze cases $\hat{k} = k^*$ and $\hat{k} \neq k^*$ separately.

1) CPEP with $\hat{k} = k^*$: In this case, the detection of transmission direction is correct, whereas the error comes from the incorrect detection of transmitted symbol, i.e., $\hat{s} \neq s^*$. Combining (7) and (8), we have

$$\mathbb{P}\big(\{k^*, s^*\} \to \{k^*, \hat{s}\}|\beta_1, \ldots, \beta_{N_s}\big) = \mathbb{P}\big(|\boldsymbol{a}_r(\theta^r_{k^*})^H \boldsymbol{n}|^2 \ > \ |\beta_{k^*}\sqrt{E}(s^* - \hat{s}) + \boldsymbol{a}_r(\theta^r_{k^*})^H \boldsymbol{n}|^2\big) = Q\Big(\sqrt{\frac{|\beta_{k^*}|^2 E|s^* - \hat{s}|^2}{2\sigma^2}}\Big) \quad (9)$$

where $Q(\cdot)$ denotes the Q-function. We omit the detailed derivation due to the page limitation.

2) CPEP with $\hat{k} \neq k^*$: In this case, the detection of transmission direction is incorrect, so that we have either $\hat{s} \neq s^*$ or $\hat{s} = s^*$. Again combining (7) and (8), we have

$$\mathbb{P}\big(\{k^*, s^*\} \to \{\hat{k}, \hat{s}\} \mid \beta_1, \ldots, \beta_{N_s}\big) = \mathbb{P}\Big(|\boldsymbol{a}_r(\theta^r_{k^*})^H \boldsymbol{n}|^2 \ > \ |\boldsymbol{a}_r(\theta^r_{\hat{k}})^H \boldsymbol{n} - \beta_{\hat{k}}\sqrt{E}\hat{s}|^2\Big) = \frac{1}{2}\exp\Big(-\frac{|\beta_{\hat{k}}|^2 E|\hat{s}|^2}{2\sigma^2}\Big). \quad (10)$$

With the conditional PEPs in (9) and (10), we derive the CBER using the union bound:

$$p_b(\beta_1, \ldots, \beta_{N_s}) \leq C_1 \sum_{k^*, s^*} \sum_{\hat{k}, \hat{s}} E_b\big(\{k^*, s^*\} \to \{\hat{k}, \hat{s}\}\big) \mathbb{P}\big(\{k^*, s^*\} \to \{\hat{k}, \hat{s}\} \mid \beta_1, \ldots, \beta_{N_s}\big) \quad (11)$$

where $C_1 \triangleq \frac{1}{N_b N(k^*, s^*)}$, and N_b is the total number of bits (included in both the direction and the symbol) transmitted every time, $N(k^*, s^*)$ denotes the total number of possible realizations of k^* and s^*, and $E_b\big(\{k^*, s^*\} \to \{\hat{k}, \hat{s}\}\big)$ is the number of erroneous bits when k^*, s^* are transmitted but $\hat{k}, \hat{s}$ are received.

Using the same example as in Section II-B, we have $N_b = 4$. For four possible transmission directions (k^*) and four possible transmitted symbols (s^*), there are total $4 \times 4 = 16$ possible realizations of pairs of k^* and s^*. Thus, $N(k^*, s^*) = 16$. If $k^* = 1, s^* = \frac{1+1j}{\sqrt{2}}\big([b_1, b_2, b_3, b_4] = [0000]\big)$, and detected $\hat{k} = 2, \hat{s} = \frac{1-1j}{\sqrt{2}}\big([\hat{b}_1, \hat{b}_2, \hat{b}_3, \hat{b}_4] = [0101]\big)$, then two bits are incorrect, so that $E_b\big(\{k^*, s^*\} \to \{\hat{k}, \hat{s}\}\big) = 2$ in this case. From the example, we see that the BER performance (11) is related to not only the CPEP of some events, but also the number of scattering clusters and the symbol modulation. The CBER of both FSSM and PSSM can be calculated using the same approach as in (11), but with different N_s and N'_s, as well as conditional variables $\beta_1, \ldots, \beta_{N_s}$ and $\beta_1, \ldots, \beta_{N'_s}$.

C. MBF

The MBF makes the UT steer to the cluster having the largest gain, i.e., β_1 in our assumption. Thus, the transmit direction vector is given by $\boldsymbol{p} = \boldsymbol{a}_t(\theta^t_1)$. For transmitted symbol s^*, the received signal at the BS is given by

$$\boldsymbol{y} = \sqrt{E}\boldsymbol{H}\boldsymbol{p}s^* + \boldsymbol{n} = \sqrt{E}\boldsymbol{a}_r(\theta^r_1)\beta_1 s^* + \boldsymbol{n}.$$

Under assumption that CSI is available at the UT and BS, the BS has knowledge about the direction of the scaterring cluster that has the largest gain. Thus, the optimal combiner would be $\boldsymbol{r} = \boldsymbol{a}_r(\theta^r_1)$. After combining, we have

$$y_c = \boldsymbol{r}^H \boldsymbol{y} = \sqrt{E}\beta_1 s^* + \boldsymbol{a}_r(\theta^r_1)^H \boldsymbol{n}.$$

ML detection of the MBF is given by

$$\begin{aligned} \hat{s} &= \arg\min_s |y_c - \boldsymbol{a}_r(\theta^r_1)^H \boldsymbol{H}\boldsymbol{a}_t(\theta^t_1)\sqrt{E}s|^2 \\ &= \arg\min_s |y_c - \sqrt{E}\beta_1 s|^2 \\ &= \arg\min_s |\sqrt{E}\beta_1(s^* - s) + \boldsymbol{a}_r(\theta^r_1)^H \boldsymbol{n}|^2. \quad (12) \end{aligned}$$

From (12), the CPEP of the MBF is derived as follows:

$$\mathbb{P}\big(s^* \to \hat{s}|\beta_1, \ldots, \beta_{N_s}\big) = \mathbb{P}\big(|\boldsymbol{a}_r(\theta^r_1)^H \boldsymbol{n}|^2 \ > \ |\beta_1\sqrt{E}(s^* - \hat{s}) + \boldsymbol{a}_r(\theta^r_1)^H \boldsymbol{n}|^2\big) = Q\Big(\sqrt{\frac{|\beta_1|^2 E|s^* - \hat{s}|^2}{2\sigma^2}}\Big). \quad (13)$$

The final CBER for the MBF is upper bounded by using union bound as:

$$p_b(\beta_1, \ldots, \beta_{N_s}) \leq \frac{1}{N_b N(s^*)} \sum_{s^*} \sum_{\hat{s}} \mathbb{P}\big(s^* \to \hat{s} \mid \beta_1, \ldots, \beta_{N_s}\big) E_b\big(s^* \to \hat{s}\big) \quad (14)$$

where N_b, $N(s^*)$, and $E_b(s^* \to \hat{s})$ denote the number of transmitted bits each time, total number of realizations of s^*, and the number of erroneous bits when s^* is transmitted but $\hat{s}$ is received.

D. Discussion

The upper bounds on the CBER for SSM and MBF are respectively given in (11) and (14). When the signal to noise ratio (SNR) is large, then the upper bounds become tight and there exists a dominant term. By the upper bound on Q function as $Q(x) \leq \frac{1}{2}e^{-\frac{x^2}{2}}$, we can have for (9) and (13) as:

$$Q\Big(\sqrt{\frac{|\beta_{k^*}|^2 E|s^* - \hat{s}|^2}{2\sigma^2}}\Big) \leq \frac{1}{2}\exp\Big(-\frac{|\beta_{k^*}|^2 E|s^* - \hat{s}|^2}{4\sigma^2}\Big), \text{and}$$
$$Q\Big(\sqrt{\frac{|\beta_1|^2 E|s^* - \hat{s}|^2}{2\sigma^2}}\Big) \leq \frac{1}{2}\exp\Big(-\frac{|\beta_1|^2 E|s^* - \hat{s}|^2}{4\sigma^2}\Big). \quad (15)$$

$$
\begin{aligned}
|\boldsymbol{y}_c(k^*) - \boldsymbol{a}_r(\theta^r_{k^*})^H \boldsymbol{H} \boldsymbol{a}_t(\theta^t_{k^*})\sqrt{E}s^*|^2 &= |\boldsymbol{a}_r(\theta^r_{k^*})^H \boldsymbol{n}|^2, \\
|\boldsymbol{y}_c(\hat{k}) - \boldsymbol{a}_r(\theta^r_{\hat{k}})^H \boldsymbol{H} \boldsymbol{a}_t(\theta^t_{\hat{k}})\sqrt{E}\hat{s}|^2 &= \begin{cases} |\boldsymbol{a}_r(\theta^r_{\hat{k}})^H \boldsymbol{n} - \beta_{\hat{k}}\sqrt{E}\hat{s}|^2, & \hat{k} \neq k^* \\ |\beta_{k^*}\sqrt{E}(s^* - \hat{s}) + \boldsymbol{a}_r(\theta^r_{k^*})^H \boldsymbol{n}|^2, & \hat{k} = k^*. \end{cases}
\end{aligned} \tag{8}
$$

As one example, we use a fixed $S = 4$ with $R = 4$. For this case, the dominant terms for each scheme can be computed as follows:

$$
\begin{aligned}
\text{FSSM}, N_s = 4, \text{QPSK} \quad &: \quad \exp\Big(-\frac{\beta_4^2 E}{2\sigma^2}\Big), \\
\text{PSSM}, N_s = 2, \text{8QAM} \quad &: \quad \exp\Big(-\frac{\beta_2^2 E}{(3+\sqrt{3})\sigma^2}\Big), \text{ and} \\
\text{MBF}, \text{16QAM} \quad &: \quad \exp\Big(-\frac{\beta_1^2 E}{10\sigma^2}\Big)
\end{aligned} \tag{16}
$$

which shows how the gain of scattering clusters, $\beta_1, \beta_2, \beta_4$ affects the performance. For example, MBF will have smaller CBER when the dominant term in MBF is smaller than SSMs, i.e., $\frac{\beta_1^2 E}{10\sigma^2} > \frac{\beta_4^2 E}{2\sigma^2}$, $\beta_1^2 > 5\beta_4^2$ for $N_s = 4$, and $\frac{\beta_1^2 E}{10\sigma^2} > \frac{\beta_2^2 E}{(3+\sqrt{3})\sigma^2}$, $\beta_1^2 > \frac{10}{3+\sqrt{3}}\beta_2^2$ for $N_s = 2$. Otherwise, the SSMs will achieve better performance than MBF. Such observation implies that each transmission scheme can have different performance when the environment changes, i.e., when $\beta_1, \beta_2, \beta_4$ take different values. The benefit of the proposed ATS comes from its ability to adaptively choose the best scheme according to the current environment, i.e., the instantaneous β_l's.

IV. Simulation Results

In this section, we present simulation results. We assume both the BS and UT have 32 antenna elements in the antenna array, $N_t = N_r = 32$. In the following figures, the curves obtained by actual link simulations are denoted by **Ex**, whereas the curves obtained by union bound are denoted by **Bound**.

There is one RF chain at the UT, whereas $R = 4$ RF chains at the BS, which implies that $N_s \leq 4$. We compare the following scheme as

1) FSSM which applies SSM with $N_s = 4$,
2) PSSM which utilizes SSM with $N_s = 2$,
3) MBF,
4) ATS which adaptively chooses one best scheme out of FSSM, PSSM, and MBF.

We assume that a gain of the scattering cluster is distributed according to $\beta_l \sim \mathcal{CN}(0, \gamma_l)$, where $\gamma_l = 10^{-0.1 z_l}$ with $z_l \sim \mathcal{N}(0, \epsilon^2), \forall l$. A variance of the scattering cluster gain is distributed according to lognormal distribution with a variance ϵ^2 [12]. The AOA and AOD of N_{ts} clusters are randomly picked from Discrete Fourier Transform (DFT) grid in order to agree with the orthogonal constraint in (2). For fair comparisons, we constrain the spectral efficiency of the system to be four bits per transmission, and have the following transmission schemes as:

Name	FSSM	PSSM	MBF	ATS
Scheme	4 clusters + QPSK	2 clusters + 8QAM	16QAM	FSSM/ PSSM/ MBF

Fig. 2 shows BER performance of different schemes with a different number of scattering clusters. This figure shows that the analytical bounds and simulation results match well for the considered schemes as the SNR increases. We assumed $\epsilon^2 = 1$ in the simulations. It shows that when $N_{ts} = 6$ and $N_{ts} = 12$, MBF achieves better average BER performance comparing to FSSM and PSSM. However, as N_{ts} increases, performance gap between MBF and SSMs becomes smaller. In all the SNR range, the ATS achieves the best performance of all.

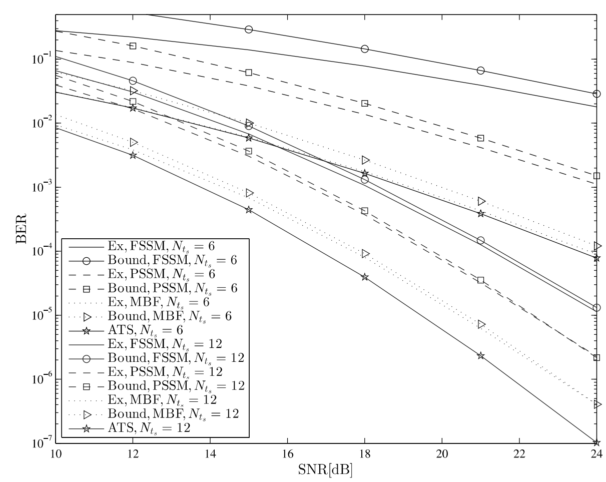

Fig. 2: BER performance for various transmission schemes with $N_{ts} = 6$ and $N_{ts} = 12$.

For the same channel model, Fig. 3 shows the impact of a large number of total scattering clusters N_{ts} on the BER. In this experiment, we set $N_{ts} = 18$. This figure shows that the existence of a larger number of total scattering clusters is more beneficial to SSM (for both FSSM and PSSM). Similar to the previous experiment with $N_{ts} = 6$, the ATS achieves the best BER performance in all the SNR range. Although the average BER of MBF is better than those of FSSM and PSSM, the ATS gets benefits from their instantaneous BER performance. Especially, $N_{ts} = 18$ provides ATS with 10 dB gain at 1×10^{-4} BER over the case of $N_{ts} = 6$.

Fig. 4 illustrates a selection probability of three non-adaptive transmission schemes for a different number of scattering clusters. This figure shows that as either the SNR

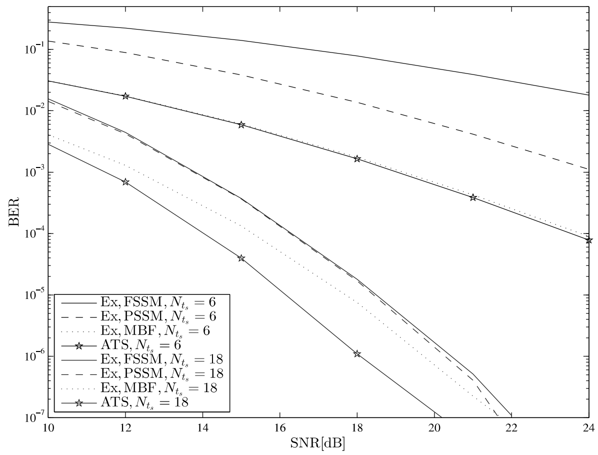

Fig. 3: BER performance for various transmission schemes with $N_{ts} = 18$.

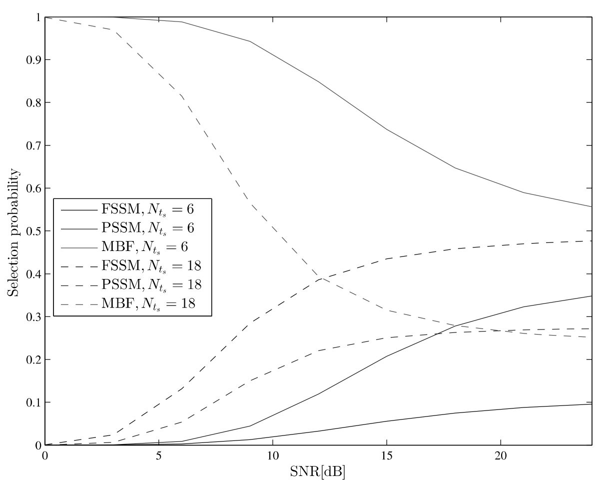

Fig. 4: Selection probability for non-adaptive transmission schemes.

or the number of scattering clusters increases, the selection opportunity for FSSM and PSSM increases. The result in Fig. 4 reflects the results in Figs. 2 and 3, where average BERs are dominated by the worst performance. When $N_{ts} = 18$, although MBF can achieve better BER performance over SSM schemes in average sense, there exist more transmission times that the SSM schemes achieve the smallest instantaneous BER. Even for $N_{ts} = 6$, there are about 45% of time that the SSM schemes (FSSM and PSSM) can achieve better instantaneous BER. This make ATS improve BER performance in all the SNR range. Simulation results also imply that the SSM schemes favor a larger number of clusters N_{ts}, so that $N_s < N_{ts}$ chosen clusters can have more similar cluster gains. From the example as shown in (16) where the dominant terms of the upper bounds are derived, when N_s clusters have similar gains, the conditions $\beta_1^2 > 5\beta_4^2$ and $\beta_1^2 > \frac{10}{3+\sqrt{3}}\beta_2^2$ are less likely to be satisfied, thus SSM schemes are more likely to achieve better performance than MBF.

V. Conclusion

In this paper, we have proposed a spatial scattering modulation scheme, which utilizes the spatial dimension to modulate additional information bits. The proposed scheme leverages the architecture of analog and hybrid beamforming, which is more practical in mmWave communications systems. Based on the derivation of CBER, we have designed the ATS, which chooses the transmission scheme that provides the best CBER at each transmission time. Simulation results have shown that the ATS achieves the best BER for all the SNR region. As the total number of scattering clusters or SNR increases, it is also shown that the ATS achieves better performance than non-adaptive transmission schemes.

References

[1] S. Sun, T. S. Rappaport, R. W. Heath, A. Nix, and S. Rangan, "Mimo for millimeter-wave wireless communications: beamforming, spatial multiplexing, or both?" *IEEE Commun. Mag.*, vol. 52, no. 12, pp. 110–121, 2014.

[2] W. Roh, J.-Y. Seol, J. Park, B. Lee, J. Lee, Y. Kim, J. Cho, K. Cheun, and F. Aryanfar, "Millimeter-wave beamforming as an enabling technology for 5g cellular communications: theoretical feasibility and prototype results," *IEEE Commun. Mag.*, vol. 52, no. 2, pp. 106–113, 2014.

[3] R. Y. Mesleh, H. Haas, S. Sinanovic, C. W. Ahn, and S. Yun, "Spatial modulation," *IEEE Trans. Veh. Technol.*, vol. 57, no. 4, pp. 2228–2241, 2008.

[4] J. Jeganathan, A. Ghrayeb, and L. Szczecinski, "Spatial modulation: optimal detection and performance analysis," *IEEE Commun. Lett.*, vol. 12, no. 8, pp. 545–547, 2008.

[5] N. Yang, P. L. Yeoh, M. Elkashlan, R. Schober, and I. B. Collings, "Transmit antenna selection for security enhancement in MIMO wiretap channels," *IEEE Trans. Commun.*, vol. 61, no. 1, pp. 144–154, Jan. 2013.

[6] M. Di Renzo, H. Haas, A. Ghrayeb, S. Sugiura, and L. Hanzo, "Spatial modulation for generalized mimo: Challenges, opportunities, and implementation," *Proceedings of the IEEE*, vol. 102, no. 1, pp. 56–103, 2014.

[7] J. Jeganathan, A. Ghrayeb, and L. Szczecinski, "Generalized space shift keying modulation for mimo channels," in *Personal, Indoor and Mobile Radio Communications, 2008. PIMRC 2008. IEEE 19th International Symposium on*. IEEE, 2008, pp. 1–5.

[8] T. L. Narasimhan, P. Raviteja, and A. Chockalingam, "Generalized spatial modulation in large-scale multiuser mimo systems," *IEEE Transactions on Wireless Communications*, vol. 14, no. 7, pp. 3764–3779, 2015.

[9] A. Kalis, A. G. Kanatas, and C. B. Papadias, "A novel approach to MIMO transmission using a single RF front end," *IEEE J. Sel. Areas Commun.*, vol. 26, no. 6, pp. 972–980, Aug. 2008.

[10] E. Başar, Ü. Aygölü, E. Panayırcı, and H. V. Poor, "Orthogonal frequency division multiplexing with index modulation," *IEEE Trans. Signal Process.*, vol. 61, no. 22, pp. 5536–5549, 2013.

[11] E. Basar, "On multiple-input multiple-output ofdm with index modulation for next generation wireless networks," *IEEE Trans. Signal Process.*, vol. 64, no. 15, pp. 3868–3878, 2016.

[12] M. R. Akdeniz, Y. Liu, M. K. Samimi, S. Sun, S. Rangan, T. S. Rappaport, and E. Erkip, "Millimeter wave channel modeling and cellular capacity evaluation," *IEEE J. Sel. Areas Commun.*, vol. 32, no. 6, pp. 1164–1179, 2014.

[13] O. El Ayach, S. Rajagopal, S. Abu-Surra, Z. Pi, and R. W. Heath, "Spatially sparse precoding in millimeter wave mimo systems," *IEEE Trans. Wireless Commun.*, vol. 13, no. 3, pp. 1499–1513, 2014.

[14] X. Zhang, A. F. Molisch, and S.-Y. Kung, "Variable-phase-shift-based rf-baseband codesign for mimo antenna selection," *IEEE Trans. Signal Process.*, vol. 53, no. 11, pp. 4091–4103, 2005.

[15] A. M. Sayeed, "Deconstructing multiantenna fading channels," *IEEE Trans. Signal Process.*, vol. 50, no. 10, pp. 2563–2579, 2002.

[16] H. L. Van Trees, *Detection, estimation, and modulation theory, optimum array processing*. John Wiley & Sons, 2004.